

## Mass enhancement and spin-glass behavior in $\text{Pr}_2\text{CuSi}_3$

Cheng Tien, Ludwig Luo, and Jih Shang Hwang

Department of Physics, National Cheng Kung University, Tainan, Taiwan, Republic of China

(Received 10 February 1997; revised manuscript received 7 July 1997)

We report magnetic-susceptibility, specific-heat, and electrical resistivity measurements of  $\text{Pr}_2\text{CuSi}_3$ . This compound exhibits ferromagnetism at  $T_c = 10$  K and upon further cooling shows spin-glass properties below about  $T_f = 8$  K. The coefficient of the term linear in temperature in the specific heat  $\gamma$  of  $\text{Pr}_2\text{CuSi}_3$  is  $0.505 \text{ J mol}^{-1} \text{ K}^{-2}$  which is much larger than that of normal metals. This compound might be classified as a nonmagnetic atom-disorder spin glass. [S0163-1829(97)00642-5]

### I. INTRODUCTION

Spin-glass magnetism could result in a possible enlargement of specific heat.<sup>1,2</sup> As an example, the  $\gamma$  value of  $\text{CePd}_3\text{B}_{0.3}$  is  $0.240 \text{ J mol}^{-1} \text{ Ce K}^{-2}$ ; so Gschneidner *et al.*<sup>3</sup> suggested that the enhancement of  $\gamma$  is due to a presence of atomic site disorder. In  $\text{CePd}_3\text{B}_{0.3}$  the B atoms randomly occupy the body-center site of this antiperovskite crystal, which introduces a varying electronic environment around Ce ions and thus causes a variation in the Ruderman-Kittel-Kasuya-Yosida mediated exchange interaction between the Ce ions. The interaction depends upon the boron occupation in the vicinity of Ce ions. It is this random Ce-Ce exchange interaction which gives rise to the spin-glass behavior and this accounts for the large observed  $\gamma$  value, where  $\gamma$  is the coefficient of the term linear in temperature in the specific heat. Gschneidner *et al.* called this phenomena nonmagnetic atom-disorder spin glasses (NMAD spin glasses).

The NMAD spin glasses  $\text{U}_2\text{TSi}_3$  ( $T = \text{Fe, Co, Ni, Ru, Rh, Pd, Os, Ir, Pt, Au}$ ) which crystallize in the hexagonal  $\text{AlB}_2$ -type structure, were reported by Kaczorowski and Noel.<sup>4</sup> The low-temperature spin-glass behavior in  $\text{U}_2\text{TSi}_3$  results from the statistical distribution of T and Si atoms at crystallographically equivalent lattice site, and gives some randomness in  $U$ - $U$  exchange interactions.

An additional  $\text{AlB}_2$ -type NMAD spin glass  $\text{CeCuSi}_3$  was reported by Hwang, Lin, and Tien.<sup>5</sup> The electric specific heat indicated a  $\gamma$  of  $0.076 \text{ J mol}^{-1} \text{ K}^{-2}$  Ce. The enhancement of  $\gamma$  could be due to the B site being occupied randomly by Si and Cu. If this argument is correct, we might also observe the spin-glass behaviors with the enhancement of  $\gamma$  in other  $\text{RE}_2\text{CuSi}_3$  compounds. In this paper, we discuss the enhancement of  $\gamma$  in  $\text{Pr}_2\text{CuSi}_3$ .

### II. EXPERIMENTAL RESULTS

Polycrystalline samples of  $\text{Pr}_2\text{CuSi}_3$  and  $\text{La}_2\text{CuSi}_3$  were prepared by the arc melting of the pure elements in their stoichiometric ratio in an atmosphere of purified argon gas. The button was flipped over and remelted a number of times to achieve good homogeneity. The overall weight loss during the melting was less than 0.1%. X-ray measurements of the sample were carried out at room temperature and showed only a single phase. Figure 1 shows the x-ray-diffraction patterns of  $\text{Pr}_2\text{CuSi}_3$  and  $\text{La}_2\text{CuSi}_3$ . The structure is consis-

tent with the hexagonal  $\text{AlB}_2$  type. The lattice parameters are  $a = 4.052 \text{ \AA}$ ,  $c = 4.255 \text{ \AA}$  for  $\text{Pr}_2\text{CuSi}_3$ , and  $a = 4.084 \text{ \AA}$ ,  $c = 4.395 \text{ \AA}$  for  $\text{La}_2\text{CuSi}_3$ .

The magnetization studies were performed in a superconducting quantum-interference device (SQUID) magnetometer. The inset of Fig. 2 is the temperature dependence of the inverse of molar susceptibility  $1/\chi$  for  $\text{Pr}_2\text{CuSi}_3$  at 50 G. The magnetic susceptibility of  $\text{La}_2\text{CuSi}_3$  is roughly three orders of magnitude smaller than that of  $\text{Pr}_2\text{CuSi}_3$ . As shown in the inset of Fig. 2, the susceptibility of  $\text{Pr}_2\text{CuSi}_3$  follows Curie-Weiss law above 15 K. Below this temperature, a negative deviation appears. The effective moment deduced from the paramagnetic region is  $3.54 \mu_B$  which is in agreement with the theoretical value of  $\text{Pr}^{3+}$  free atom at  $^3\text{H}_4$  state. Below 10 K,  $\text{Pr}_2\text{CuSi}_3$  is ferromagnetic. Figure 2 is the susceptibilities

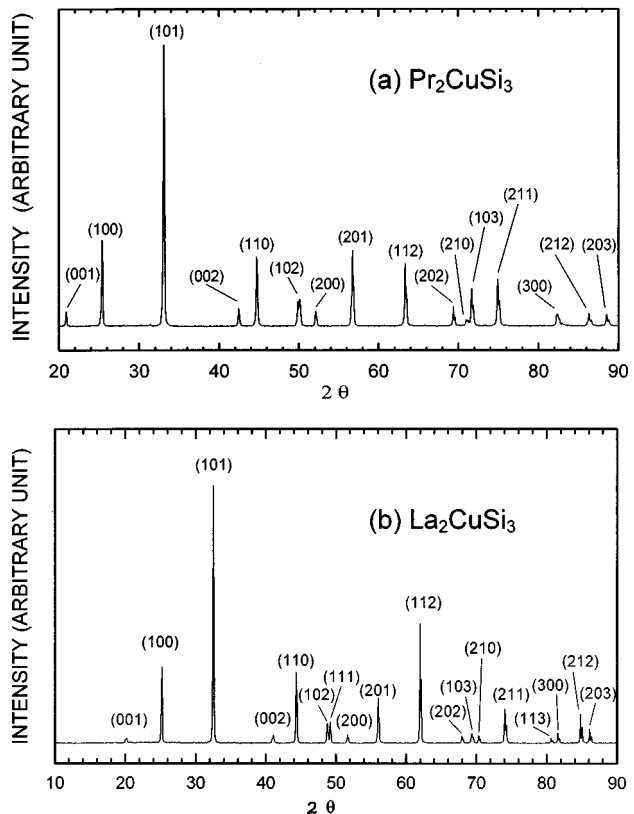


FIG. 1. The x-ray-diffraction patterns of  $\text{Pr}_2\text{CuSi}_3$  and  $\text{La}_2\text{CuSi}_3$ .

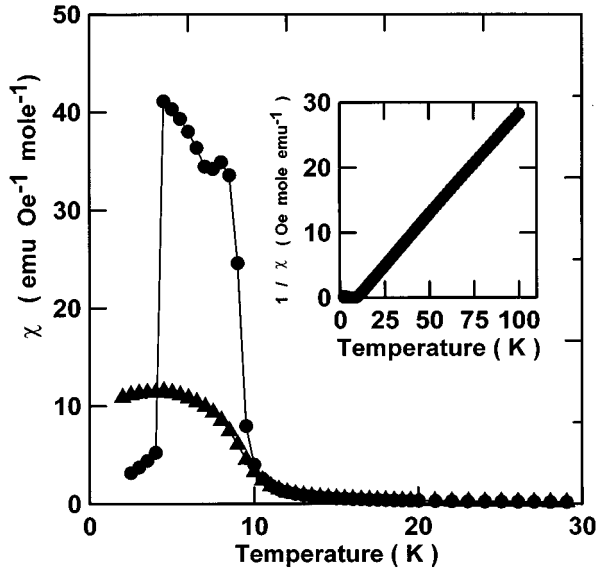


FIG. 2. The susceptibilities of  $\text{Pr}_2\text{CuSi}_3$  between 2 and 30 K in 50 G (●) and 1000 G (▲). The inset is the temperature dependence of the inverse of molar susceptibility  $1/\chi$  for  $\text{Pr}_2\text{CuSi}_3$  at 50 G.

of  $\text{Pr}_2\text{CuSi}_3$  between 2 and 30 K in 50 and 1000 G. The method to measure the susceptibility is the zero-field-cooling (ZFC). We cooled the sample from 300 to 2 K in the zero field and applied the field at 2 K. Then we heated the sample while measuring the magnetization  $M$  within the constant field. In 50 G, there is a ferromagnetic transition at 10 K but the magnetization at 2 K is much smaller than that at 8 K. A small peak was observed at 8.5 K. A similar behavior was observed in  $\text{U}_2\text{NiSi}_3$ .<sup>6</sup> This 8.5 K peak will be smeared out in 1000 G. However, even in 1000 G, the magnetization at 2 K in a zero-field-cooling process is still smaller than that at 8 K. The field dependencies of the magnetization  $M(H)$  of  $\text{Pr}_2\text{CuSi}_3$  at 20, 10, 8, and 2 K are shown in Fig. 3. Below 10 K, the magnetization curves clearly deviate from a linear relationship between  $M$  and  $H$ . As shown in Fig. 3, there is

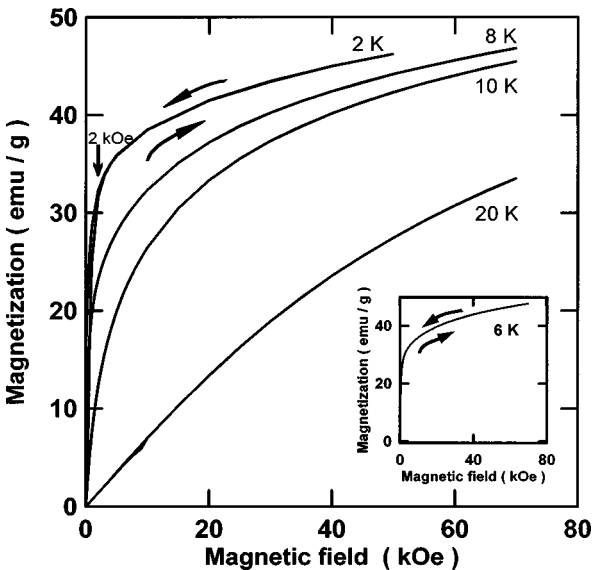


FIG. 3. The field dependence of the magnetization  $M(H)$  of  $\text{Pr}_2\text{CuSi}_3$ , at 20, 10, 8, and 2 K. The inset is  $M(H)$  at 6 K.

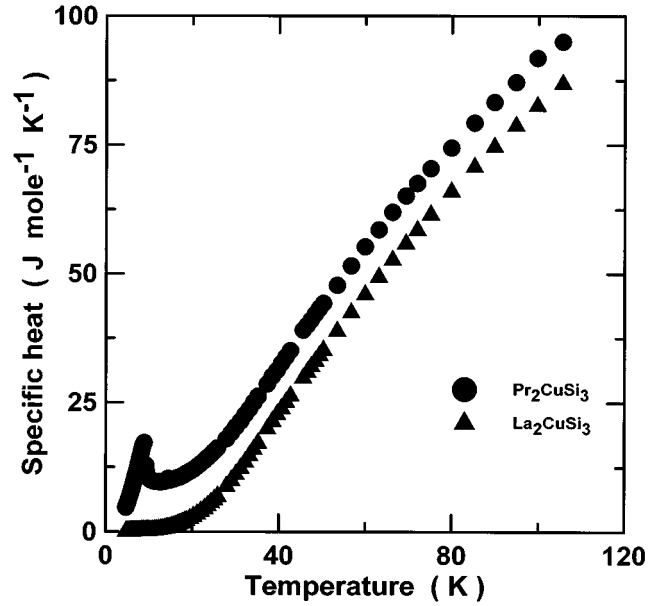


FIG. 4. The specific heat versus temperature  $C(T)$  of  $\text{Pr}_2\text{CuSi}_3$  and  $\text{La}_2\text{CuSi}_3$ .

no hysteresis or remanent magnetization at 20, 10, and 8 K. However, as shown in Fig. 3, the  $M(H)$  at 6 and 2 K show remanent magnetization and hysteresis.

The specific-heat measurements were performed in an adiabatic calorimeter by a modified heat-pulse method.<sup>7</sup> Figure 4 gives the specific heat versus temperature  $C(T)$  of  $\text{Pr}_2\text{CuSi}_3$  and  $\text{La}_2\text{CuSi}_3$ . The peak of  $C(T)$  indicates a phase transition in  $\text{Pr}_2\text{CuSi}_3$  near 8 K. Below 40 K the  $C(T)$  of  $\text{La}_2\text{CuSi}_3$  can be described by  $C(T) = \gamma_1 T + \beta_1 T^3$  with  $\beta_1 = 0.344 \times 10^{-3} \text{ J mol}^{-1} \text{ K}^{-4}$  and  $\gamma_1 = 5.61 \times 10^{-3} \text{ J mol}^{-1} \text{ K}^{-2}$ . Between 20 and 40 K, the  $C(T)$  of  $\text{Pr}_2\text{CuSi}_3$  can be fitted by  $C(T) = \gamma_2 T + \beta_2 T^3$  with  $\beta_2 = 0.184 \times 10^{-3} \text{ J mol}^{-1} \text{ K}^{-4}$  and  $\gamma_2 = 0.509 \text{ J mol}^{-1} \text{ K}^{-2}$ . The magnetic specific heat is defined here as  $C_m(T) = C(\text{Pr}_2\text{CuSi}_3)$

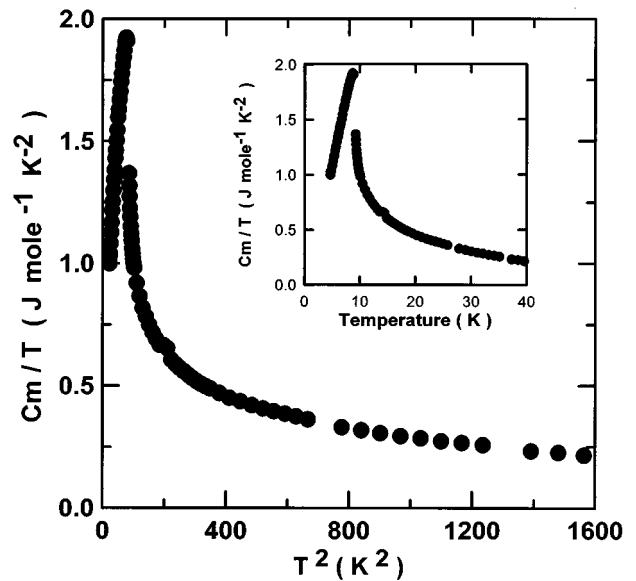


FIG. 5. The  $C_m/T$  versus  $T^2$  of  $\text{Pr}_2\text{CuSi}_3$  between 20 and 40 K. The inset is  $C_m/T$  versus  $T$ .

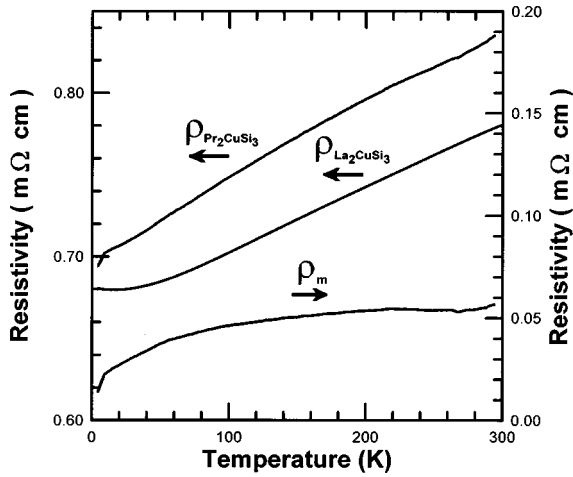


FIG. 6. The electrical resistivities of  $\text{Pr}_2\text{CuSi}_3$  and  $\text{La}_2\text{CuSi}_3$  versus temperature between 4.2 and 300 K. The magnetic resistivity  $\rho_m(T)$  of  $\text{Pr}_2\text{CuSi}_3$  is defined as  $\rho_m(T) = \rho(\text{Pr}_2\text{CuSi}_3) - \rho(\text{La}_2\text{CuSi}_3)$ .

$-C(\text{La}_2\text{CuSi}_3)$ . The  $C_m/T$  versus  $T^2$  is shown in Fig. 5. Between 20 and 40 K,  $C_m(T)/T = \gamma + \beta T^2$  with  $\beta = 0.200 \times 10^{-3} \text{ J mol}^{-1} \text{ K}^{-4}$  and  $\gamma = 0.505 \text{ J mol}^{-1} \text{ K}^{-2}$ . It is seen that  $\gamma \cong \gamma_1 - \gamma_2$  and  $\beta \cong \beta_1 - \beta_2$ . The temperatures of our specific-heat measurements are not low enough to determine the entropy accurately. The corresponding  $C_m/T$  versus  $T$  is shown in the inset of Fig. 7. A rough estimate of the magnetic entropy is  $18.95 \text{ J K}^{-1} \text{ mol}^{-1}$  which is only about half of  $2R \ln 9$ .

The electrical resistivities of  $\rho(T)$  of  $\text{Pr}_2\text{CuSi}_3$  and  $\text{La}_2\text{CuSi}_3$  between 4.2 and 300 K are shown in Fig. 6. The resistivity of  $\text{Pr}_2\text{CuSi}_3$  decreases linearly with decreasing temperature down to 8 K. At 8 K the slope of  $\rho(T)$  changes. The quick reduction of  $\rho(T)$  which corresponds to the 8-K peak in specific-heat measurements also suggests a phase transition at 8 K.

### III. DISCUSSION

The  $\gamma$  of  $\text{Pr}_2\text{CuSi}_3$  is  $0.505 \text{ J mol}^{-1} \text{ K}^{-2}$  which is much larger than those of normal metals. Praseodymium compounds usually do not form heavy-fermion materials. However, a strong Kondo Fermi-liquid state has been recently observed in  $\text{PrInAg}_2$ .<sup>8</sup>

The temperature dependence of resistivity of  $\text{Pr}_2\text{CuSi}_3$  is similar to that of  $\text{PrInAg}_2$ . The resistivity may be considered a consequence of the following contribution:

$$\rho(T) = \rho_{\text{imp}} + \rho_{\text{ph}}(T) + \rho_m(T),$$

where  $\rho_{\text{imp}}$  is due to the scatter of impurities and lattice imperfections,  $\rho_{\text{ph}}(T)$  is the contribution due to the electron-phonon interaction, and any other scattering mechanism is contained in  $\rho_m(T)$ . Since, in the specific heats the lattice

contributions of  $\text{Pr}_2\text{CuSi}_3$  and  $\text{La}_2\text{CuSi}_3$  are roughly identical,  $\rho_{\text{ph}}(T)$  of both compounds might be also the same. Therefore,

$$\rho_m(T) \cong \rho(\text{Pr}_2\text{CuSi}_3) - \rho(\text{La}_2\text{CuSi}_3).$$

Between 300 and 100 K,  $\rho_m(T)$  slowly decreases with decreasing temperature. The fall of  $\rho_m(T)$  at  $\sim 50$  K might indicate correlated electrons. Although the specific heat of  $\text{Pr}_2\text{CuSi}_3$  exhibits heavy-fermion behavior, the resistivity is uncharacteristic. For example, there is no evidence of logarithmic increase of  $\rho(T)$  with decreasing temperature and there is no indication of a coherence peak. However, we still cannot rule out this possibility.

As indicated in Fig. 4, there is no Schottky-type anomaly between 4.2 and 100 K. Although we could not exclude such a possibility at high temperature, the crystal field levels larger than 100 K will not contribute to the low-temperature heat capacity. Therefore, except for the heavy-fermion mechanism, the possible mechanisms that will enhance the  $\gamma$  value are (1) low-lying crystal levels or magnetic ordering at very low temperature, or (2) the nonmagnetic-atom-disorder-spin-glass (NMAD-spin-glass) behavior suggested by Gschneidner *et al.*<sup>3</sup>

The lattice parameters of  $\text{Pr}_2\text{CuSi}_3$  are nearly the same as those of the corresponding hexagonal  $\text{PrSi}_2$ . According to the argument of Chevalier *et al.*,<sup>6</sup> in the  $\text{AlB}_2$  type of  $\text{Pr}_2\text{CuSi}_3$ , Pr is in the Al-site; Si and Cu occupy the B-site randomly.  $\text{Pr}^{3+}$  ions are located on the layers separated by sheets composed of Si and Cu atoms. The randomness of Si and Cu introduces a varying electron environment around the Pr ions. It is these random Pr-Pr exchange interactions that give rise to the spin-glass behavior, and this accounts for the large observed  $\gamma$  value.

Therefore, as indicated in Fig. 2, the drop in of  $\chi(T)$  at low temperature can be interpreted as follows: When  $\text{Pr}_2\text{CuSi}_3$  is cooled from 300 to 2 K in zero field, it will form a spin-glass ordering; therefore, below a characterized temperature  $T_f$ ,  $\chi(T) \sim 0$ . The steep increase in susceptibility at 4.2 K is an anomaly due to the magnetometer.

Studying the spin glass by SQUID technique was discussed by Mydosh.<sup>9</sup> First, we cooled the  $\text{Pr}_2\text{CuSi}_3$  sample in the zero field to 4.5 K and applied a 5-G magnetic field at 4.5 K. Then we heated the sample while measuring the susceptibility  $\chi(T)$  to 20 K (ZFC). Second, we cooled the sample back down from 20 to 4.5 K in a 5-G field while recording  $\chi(T)$  (FC). After a ZFC and a FC processes  $\chi(T)$  was measured by cycling the temperature back and forth in a 5-G field. Figure 7 illustrates the temperature dependence of  $\chi(T)$  for  $\text{Pr}_2\text{CuSi}_3$  in a 5-G field in the different cooling process (FC versus ZFC). If  $T_g$  is defined by the onset of difference between FC and ZFC,  $T_g \cong 9$  K. As indicated in Fig. 7, the FC susceptibility traces the same path in cooling and warming processes. When the magnetic field increases, the spin-glass state will depress. The  $T_g$  is  $\sim 4$  K in a 1000 G. In a spin-glass state, it takes many decades to turn the magnetic moments toward the field direction. Even after 4 h, the magnetic moment of  $\text{Pr}_2\text{CuSi}_3$  is still not saturated.

The hysteresis of  $M(H)$  at 2 K (Fig. 3) might be also due to the time dependence of  $M(H)$  in a spin-glass state. If this

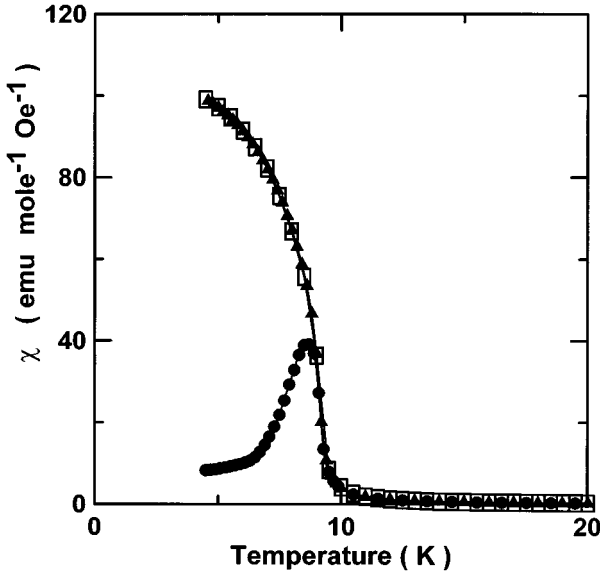


FIG. 7. The temperature dependence of  $\chi(T)$  for  $\text{Pr}_2\text{CuSi}_3$  at a 5-G field, the sample was cooled in the zero field and applied the field at 4.5 K. We heated the sample while measuring the magnetization  $M$  from 4.5 to 300 K (●), and then cooled the sample from 300 to 4.5 K (□), and finally heated the sample again from 4.5 to 300 K (▲) within the constant field.

argument is correct, the spin-glass behavior of  $\text{Pr}_2\text{CuSi}_3$  will be apparent even if the field is above 2 KOe.

Two uranium compounds  $\text{U}_2\text{NiSi}_3$  and  $\text{U}_2\text{CoSi}_3$  that have the hexagonal  $\text{AlB}_2$  structure also display ferromagnetic and spin-glass-like behaviors. Kaczorowski and Noel<sup>4</sup> reported that  $\text{U}_2\text{CoSi}_3$  first exhibited a ferromagnetism at  $T_c = 10$  K and then showed spin-glass-like properties below about  $T_f = 8$  K. The  $T_c$  and the  $T_f$  of  $\text{U}_2\text{CoSi}_3$  are 25, 22 K, respectively. Although the structure of  $\text{U}_2\text{CuSi}_3$  is the tetragonal  $\alpha\text{-ThSi}_2$ , this compound will also have ferromagnetic and spin-glass properties with  $T_c = 30$  K and  $T_f = 26$  K. This kind of compound is called reentrant spin glass or ferroglass.<sup>10,11</sup> However, there is no persuasive theorem to explain why magnetic moments will lose the arrangement and transfer from a ferromagnetic ordering to a spin-glass-like state. In a low magnetic field (5 G), the  $T_c$  and the  $T_f$  of  $\text{Pr}_2\text{CuSi}_3$  are 10, 8 K, respectively. However, without magnetic field, there is no spontaneous magnetic ordering in  $\text{Pr}_2\text{CuSi}_3$ . Therefore, in the zero magnetic field,  $\text{Pr}_2\text{CuSi}_3$  is a simple spin glass instead of a reentrant spin glass. An alternative to a loss of ferromagnetism at the spin-glass transition is the freezing of ferromagnetic domains. The very low-field susceptibility measurement might clarify this argument.

In  $\text{Pr}_2\text{CuSi}_3$ ,  $\text{Pr}^{3+}$  ions are located on layers separated by sheets of Si and Cu atoms. The possible mechanism of the spin glass in  $\text{Pr}_2\text{CuSi}_3$  is that at 8 K, the magnetic moments of  $\text{Pr}^{3+}$  ions on a same layer form a ferromagnetic order, but there is no magnetic correlation between two different  $\text{Pr}^{3+}$  layers. Below 8 K, different  $\text{Pr}^{3+}$  layers correlate antiferromagnetically. After a magnetic field is applied, the competition between Pr-Pr interaction and Pr-field interaction accounts for the reentrant-spin-glass property in  $\text{Pr}_2\text{CuSi}_3$ .

Although there is no magnetic correlation between two different  $\text{Pr}^{3+}$  layers, the magnetic moments of all layers will

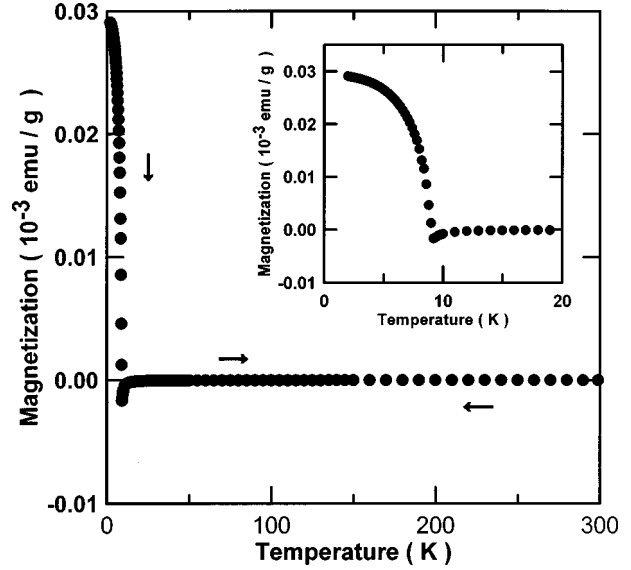


FIG. 8. The temperature dependence of magnetization  $M(T)$  in a zero magnetic field. The inset is  $M(T)$  between 2 and 20 K.

be not canceled entirely. We may still observe a ferromagnetic phase. Below 8 K, different  $\text{Pr}^{3+}$  layers correlate antiferromagnetically. Therefore, if this argument is correct, we should observe a very small spontaneous ferromagnetic ordering and an antiferromagnetic ordering in a zero magnetic field. The mass of the sample for spontaneous ferromagnetic ordering is 0.084 57 g; therefore, there are  $N = 2.37 \times 10^{20}$   $\text{Pr}^{3+}$  ions in the sample. The effective moment of each  $\text{Pr}^{3+}$  ion is  $\mu_{\text{eff}} = 3.54 \mu_B$ , such that  $N \mu_{\text{eff}} = 7.78$  emu and magnetization  $M(0) = 92.0$  emu/g. Figure 8 is the temperature dependence of magnetization  $M(T)$  in a zero magnetic field. As shown in Fig. 8, there is a very small [ $M(2 \text{ K}) = 0.03$  emu/g] spontaneous ferromagnetic ordering at  $\sim 9$  K. Below 7 K, the tendency of increase of  $M(T)$  is significantly reduced, which is consistent with an antiferromagnetic ordering among  $\text{Pr}^{3+}$  layers. Further experiments, for example, neutron scattering, are needed to characterize the unusual properties of  $\text{Pr}_2\text{CuSi}_3$ .

#### IV. CONCLUSIONS

The structure of  $\text{Pr}_2\text{CuSi}_3$  is consistent with the hexagonal  $\text{AlB}_2$  type.  $\text{Pr}_2\text{CuSi}_3$  is ferromagnetic with a Curie temperature of 10 K. At low temperature,  $\text{Pr}_2\text{CuSi}_3$  exhibits clear spin-glass behaviors. In a magnetic field above 2 KOe, the spin-glass behavior still exists.

The  $C(T)$  of  $\text{Pr}_2\text{CuSi}_3$  can be fitted by  $C(T) = \gamma_2 T + \beta_2 T^3$ , with  $\beta_2 = 1.84 \times 10^{-4} \text{ J mol}^{-1} \text{ K}^{-4}$  and  $\gamma_2 = 0.509 \text{ J mol}^{-1} \text{ K}^{-2}$ . The  $\gamma_2$  of  $\text{Pr}_2\text{CuSi}_3$  is much larger than those of normal metals. The magnetic entropy is about  $19 \text{ J K}^{-1} \text{ mol}^{-1}$  which is only about half of  $2R \ln 9$ . The magnetic entropy much less than  $2R \ln 9$  will further support the reality of spin-glass state. This compound might be classified as a nonmagnetic atom-disorder spin glass.

#### ACKNOWLEDGMENT

This work was supported by the National Science Council of Republic of China under Contract No. NSC86-2112-M-006-012.

- <sup>1</sup>W. P. Beyermann, M. F. Hundley, P. C. Canfield, J. D. Thompson, M. Latroche, C. Godart, M. Selsane, Z. Fisk, and J. L. Smith, *Phys. Rev. B* **43**, 13 130 (1991).
- <sup>2</sup>T. Takabatake, F. Teshima, H. Fujii, N. Nishigori, T. Suzuki, T. Fujita, Y. Yamaguchi, and Sakurai, *J. Magn. Magn. Mater.* **90/91**, 474 (1990).
- <sup>3</sup>K. A. Gschneidner, Jr., J. Tang, S. K. Dhar, and A. Goldman, *Physica B* **163**, 507 (1990).
- <sup>4</sup>D. Kaczorowski and H. Noel, *J. Phys.: Condens. Matter* **5**, 9185 (1993).
- <sup>5</sup>Jih Shang Hwang, K. J. Lin, and Cheng Tien, *Solid State Commun.* **100**, 169 (1996).
- <sup>6</sup>B. Chevalier, P. Lejay, J. Etourneau, and P. Hagenmuller, *Solid State Commun.* **49**, 753 (1984).
- <sup>7</sup>J. S. Hwang, K. J. Lin, and C. Tien, *Rev. Sci. Instrum.* **68**, 94 (1997).
- <sup>8</sup>A. Yatskar, W. P. Beyermann, R. Movshovich, and P. C. Canfield, *Phys. Rev. Lett.* **77**, 3637 (1997).
- <sup>9</sup>J. A. Mydosh, *Spin Glass: An Experimental Introduction* (Taylor & Francis, London, 1993).
- <sup>10</sup>R. B. Goldfarb, F. R. Fickett, K. V. Rao, and H. S. Chen, *J. Appl. Phys.* **53**, 7687 (1982).
- <sup>11</sup>R. B. Goldfarb, K. V. Rao, and H. S. Chen, *Solid State Commun.* **54**, 799 (1985).